

Tuneable Emission of POSS-based nanostructures self-assembled in presence of Eu^{3+} ions: reversible trans-to-cis isomerization

Valerio Cinà,^[ab] Esther Carbonell,^{*[a]} Luca Fusaro,^[a] Hermenegildo Garcia,^[c] Michelangelo Gruttadauria,^[b] Francesco Giacalone,^{*[b]} Carmela Aprile^{*[a]}

Dedication ((optional))

Abstract: Hybrids nanostructures with switchable and reversible “blue-red-green” emission were efficiently synthesized. The Polyhedral Oligomeric Silsesquioxane (POSS) behaves as a directional nano-brick for the organic ligands allowing an easy complexation of Europium (III) cations. The complexes were characterized via UV-Vis and fluorescence spectroscopies and the stoichiometry was also confirmed via ^1H NMR investigation. The octafunctionalized nano-cages allow forming novel self-assembled 3D architectures in presence of the lanthanide cation displaying a red-emission of particular intensity especially in solid state. The presence of a vinyl group bridging the inorganic core to the organic moiety was employed to tune the emission properties via *trans-cis* isomerization of the double bond. This behaviour, together with the easy dispersion of the dry powder and the possibility of coating it as a film in presence of small amount of solvent, makes the emitting solid promising for applications in materials science.

Introduction

Main Text Paragraph Polyhedral Oligomeric Silsesquioxane (POSS, T_8) with their cubic symmetry represents an ideal building block for the construction of 3D networks. POSS exhibits an inner inorganic nanocage surrounded by eight organic moieties, which can be easily functionalized thus offering a wide range of possibilities for the synthesis of novel hybrid solids.^[1] POSS nanostructures have attracted an increasing interest in recent decades. Due to their exceptional features, they found application in several fields from catalysis^[2] to polymer^[3] sciences. Imidazolium functionalized POSS nanostructures were efficiently employed as catalysts in the

conversion of CO_2 ^[4] or as support for Pd^[5] nanoparticles. The exceptional chemical-physical characteristics of the nanocage (rigidity and thermal stability) were also exploited to improve the thermal stability of various polymers.^[6] POSS functionalized with proper fluorophores^[7] successfully acted as nanosensors for the detection of toxic industrial chemicals and chemical warfare agent simulants, whereas when the POSS rigid core is endowed with mesogenic moieties, the resulting hybrids show liquid crystal properties.^[8] We recently proposed the use of POSS-based nanocages functionalized with terpyridine moieties as efficient nanostructure for the formation of luminescent metallopolymer in presence of Zn^{2+} and Fe^{2+} cations.^[9] Moreover, it was also described by Cheng et al. that when POSS units are functionalized with fluorescent dyes, the resulting materials display an efficient emission intensity due to a combination of the improved dispersion of the fluorophore together with the increased thermal stability as a consequence of the inorganic core.^[10]

Due to their peculiar luminescent properties, lanthanides trivalent ions (Ln(III)) and in particular Eu, Tb and Yb, have attracted the raising attention of the scientific community for the design of advanced functional materials^[11] with possible applications in fields as different as electronics or bio-medicine.^[12] The unique properties of Ln(III) include long-lived excited states, sharp line-like emission bands and large Stokes shifts. However, direct excitation of these cations is hardly obtained without laser sources due to the strongly forbidden character of the *f-f* transitions. For this reason, a species able to absorb photons at short wavelength and transfer the energy to the lanthanides, which emit lights at much longer wavelength, is normally used. This process is called “antenna effect”. Terpyridine-based ligands are largely employed for this purpose because of their light-harvesting antenna effect combined with high-affinity metal-bindings.^[13] Moreover, it is known, that independently from the ligand used, the local chemical environment has a strong influence on the emission of Ln(III) .^[14] On the other side, it would be interesting to have systems in which a controlled and tuneable emission can be obtained only via slightly chemical modification of the structure of the ligand not requiring an ex-novo synthesis pathway. For this purpose, the photochemical *cis-trans* isomerization of double bonds (vinyl, stilbene and azo compounds), have been the subject of a large variety of investigations. In some cases configurational changes can be associated with different fluorescence emissions regulated by the photoisomerization process, as well as even

[a] a. V. Cinà, Dr. E. Carbonell, Dr. L. Fusaro, Prof. C. Aprile
Laboratory of Applied Material Chemistry (CMA), University of
Namur, 61 rue de Bruxelles 5000 Namur (Belgium)
E-mail: carmela.aprile@unamur.be

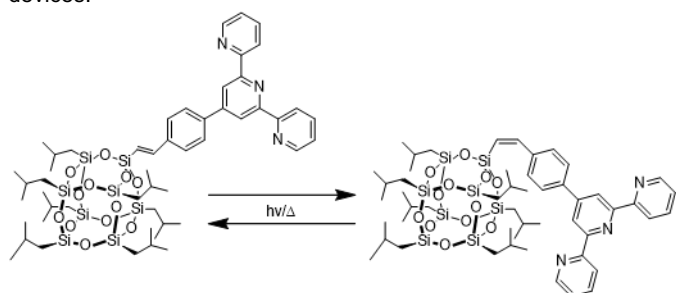
[b] b. V. Cinà, Prof F. Giacalone, Prof M. Gruttadauria
Department of Biological, Chemical and Pharmaceutical Sciences
and Technologies, University of Palermo, Viale delle Scienze, Ed.
17, 90128, Palermo (Italy)
E-Mail: francesco.giacalone@unipa.it

[c] Prof H. Garcia
Department of Chemistry, Instituto de Tecnología Química CSIC-
UPV, Universitat Politècnica de València, Av. de los Naranjos s/n,
Valencia, 46022, Spain

Supporting information for this article is given via a link at the end of
the document. ((Please delete this text if not appropriate))

on/off fluorescent switching^[15] and photostabilization^[16] via reversible *cis-trans* isomerization.^[17]

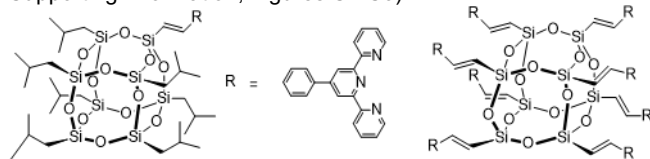
To the best of our knowledge, photoisomerization studies in presence of POSS-based hybrid materials have never been carried out. Herein, two novel Eu³⁺ complexes are proposed, employing as ligands POSS nanostructures functionalized with one (**M-POSS**) or eight (**O-POSS**) terpyridine moieties. The reversible *trans* to *cis* isomerization of the carbon-carbon vinyl moiety connecting the POSS nanocage to the terpyridine ligand is presented (Scheme 1). The **O-POSS** architectures display a switchable blue-green emission as consequence of the configurational changes. This switchable behaviour is even more evident in presence of Eu species. In this case a reversible "blue-red-green" emission can be easily achieved making the **O-POSS**-based Eu(III) complex an extremely promising and innovative material for organic-inorganic hybrid emitting devices.^[18]



Scheme 1. *Trans-cis* isomerization of **M-POSS**

Results and Discussion

The synthesis of functionalized Polyhedral Oligomeric Silsesquioxane (POSS) with 4'-phenyl-2,2':6',2''-terpyridine units was achieved via Heck coupling reaction following a procedure previously described in our research group.^[9] The structure of the corresponding mono- (**M-POSS**) and octa-functionalized POSS (**O-POSS**) is presented in Scheme 2. Both **M-** and **O-POSS** were characterized via ¹H-, ¹³C- and ²⁹Si-NMR (see Supporting Information, Figures S1-S6).



Scheme 2. Functionalized **M-POSS** and **O-POSS**.

Due to the notable light-emitting performance of the lanthanides, our attention was focused to this series of cations in order to form binary metal complexes (in presence of **M-POSS**) or 3D supramolecular assemblies (with **O-POSS**) generated through coordination of the POSS-based nanostructures with the selected metal. In particular, Eu trivalent ions were selected as target cations since they exhibit intense emission from *f-f* electronic transitions. Moreover, both POSS structures depicted in Scheme 2 display a *trans* carbon-carbon double bond that can

be isomerized to the *cis* form with important implication for both emission and coordinating properties.

Prior to the investigation of the luminescent behaviour as function of the *trans-cis* isomerization, the stoichiometry of the Eu@POSS complexes (both mono- and octa-functionalized) was addressed selecting the **M-POSS** as initial benchmark. Quantitative information on the stoichiometry of the complex in function of increasing amount of Eu(III) were obtained via ¹H NMR titration experiments (Figure S7). The variations of the normalized integrated areas of selected signals upon addition of increasing amounts of Eu(OTf)₃ are reported in Figure 1a. A progressive disappearance of the **M-POSS** free ligand contribution was observed after addition of increasing amount of Eu(III). The characteristic terpyridine signals (at 8.5 ppm), labelled with a black square, were followed for this investigation. The complete disappearance of these signals was achieved in correspondence of 0.5 eq of Eu³⁺. This result suggests the formation of a complex characterized by a metal to ligand stoichiometry of 1:2 (**Eu@2-MPOSS**). It should be mentioned that a novel pattern of signals corresponding to the formation of the terpyridine-Eu(III) complex (red circles) was evident immediately after the first additions of Eu(III) (see Figures 1a and S7). In the presence of an excess of Eu(OTf)₃ an additional set of signals appears (blue triangles) which can be reasonably attributed to the formation of the 1:1 complex (**Eu@M-POSS**).

The complexation properties of the **O-POSS** in presence of Eu(III) species was assessed as well. ¹H NMR spectrum of **O-POSS** shows a very broad band in the aromatic region due to the π - π stacking interactions (Figure S4) between the terpyridine units, as reported previously.^[9] Hence, the formation of the Eu(III) complex was indirectly followed by monitoring the disappearance of the ¹H bands upon addition of Eu(OTf)₃ (Figure S8). The complete disappearance of the ¹H contributions was achieved in correspondence of 0.5 equivalents Eu(OTf)₃ (Figure 1b) thus indicating the formation of 1:2 complex (**Eu@2O-POSS**) as previously observed when **M-POSS** was selected as ligand. Considering that lanthanides cations can accommodate up to nine coordinating atoms, the formation of complexes characterized by a metal to ligand stoichiometry of 1:2 could be considered as a consequence of the steric hindrance of the POSS nanostructure and indicates that the coordination shell of Eu(III) is only partially completed by the terpyridine moieties. Interestingly, a more detailed analysis of the aliphatic region in the ¹H NMR spectrum of **O-POSS** evidenced the shift of another signal at 1.9 ppm during the titration experiments (Figure S8).

This signal could be attributed to the presence of water molecules completing the first coordination shell of the Eu cations. It deserves to be mentioned that no signals corresponding to free terpyridine moieties were observed after titration. This evidence allows confirming that water plays only the role of co-ligand completing the coordination sphere and it is not able to promote the removal of the terpyridine moieties. The formation of both **M-POSS** and **O-POSS** based Eu(III) complexes was also followed by monitoring the changes in the absorption and fluorescence spectra.

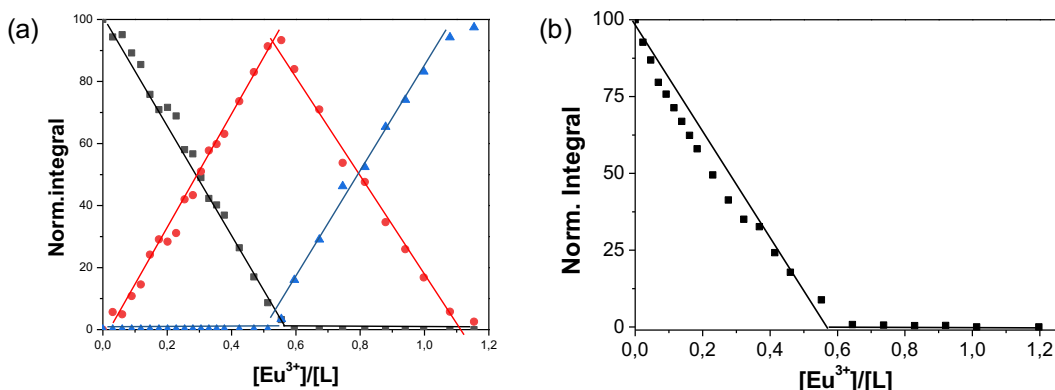


Figure 1. Changes in normalized integrated areas of selected signals of ^1H NMR titration experiments in $\text{CD}_3\text{Cl}:\text{CD}_3\text{CN}$ (7:3) of (a) M-POSS (b) O-POSS upon addition of 0-1.2 equivalents of $\text{Eu}(\text{OTf})_3$ (■ = free ligand; ● = 1:2 complex; ▲ = 1:1 complex) Line connecting the point in the plot are guides for the eyes.

Upon addition of $\text{Eu}(\text{OTf})_3$ to a solution of **M-POSS**, the absorption band at 290 nm corresponding to the $\pi-\pi^*$ transition of the terpyridine decreases remarkably. Concomitantly, the appearance of a novel absorption band above 330 nm was progressively observed (see Figure 2a). These absorption bands can be attributed to the metal/ligand complex. A plateau was reached in correspondence of a M/L ratio equal to 0.5 (inset Figure 2a) further confirming the formation of the **Eu@2M-POSS**. The fluorescence spectra followed a similar trend. As expected, the emission band of the terpyridine in the **M-POSS** ($\lambda_{\text{max.}} = 365$ nm) was completely quenched upon addition of 0.5 equivalents of metal cations (see Figure 2b). As a direct consequence of complex formation, a new emission band at $\lambda_{\text{max.}}$ ca. 455 nm was observed. This broad emission band can be attributed to the ligand-centered transitions. However, under the selected conditions, the characteristic Eu(III) emission (in the region between 550 – 700 nm) was not detected. This behaviour could

be attributed to the incomplete energy transfer from the terpyridine to the europium and/or the influence of the solvent polarity as well as the presence of water molecules. **M-POSS** possess seven hydrophobic isobutyl groups surrounding the nanocage with consequent generation of a “hydrophobic shell” influencing the self-association process.^[19] In order to better understand the reason behind the absence of this emission, a novel set of experiments employing a mixture of solvents of different polarity ($(\text{CH}_3\text{CN}$ (97%): CH_2Cl_2 (3%)) was performed as well. Figure S9 shows a non-resolved emission centered at 617 nm clearly visible in the novel mixture of solvent thus confirming the role played by the solvent on the emission of **M-POSS** structures.

However, a different behaviour with an improved emission should be expected in presence of **O-POSS** based ligands in which the isobutyl groups are replaced by terpyridine moieties.

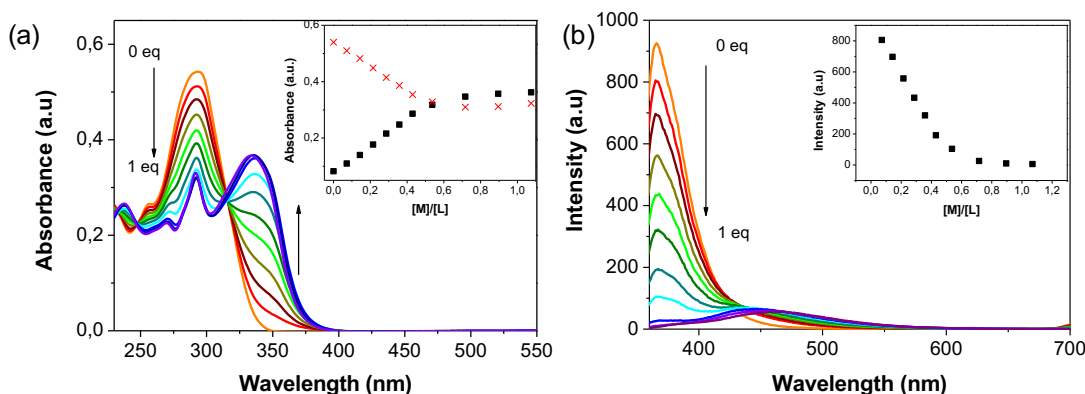


Figure 2. (a) UV-vis absorption spectra of **M-POSS** in CH_2Cl_2 (1.3×10^{-5} M) upon titration with $\text{Eu}(\text{OTf})_3$ in CH_3CN (1.4×10^{-3} M). Inset shows the normalized absorption changes at 290 nm (red crosses) and 330 nm (black squares). (b) Emission spectra of **M-POSS** in CH_2Cl_2 upon titration with $\text{Eu}(\text{OTf})_3$: 0 eq. - 1 eq. $\lambda_{\text{ex}} = 310$ nm $\text{OD}_{315\text{ nm}} = 0.27$ slits 2.5-5 and band pass filter (360 – 100 nm). Inset shows the fluorescence intensity at 366 nm

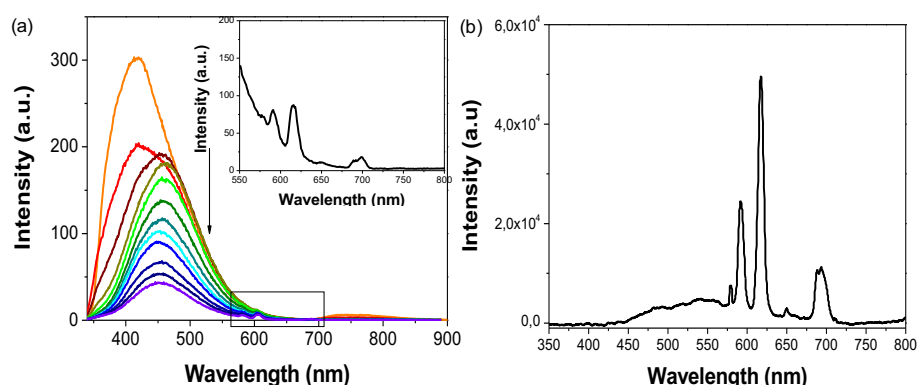


Figure 3. (a) Emission spectra of **O-POSS** [1×10^{-5} M] in CH_2Cl_2 upon addition of $\text{Eu}(\text{OTf})_3$ [1.4×10^{-3} M] in CH_3CN ($\lambda_{\text{ex}} = 313$ nm OD= 0.15 slits 5 nm). Inset shows the characteristic $\text{Eu}(\text{III})$ line-like emission. (b) Emission spectra of the **Eu@O-POSS** in solid state

As expected, the addition of $\text{Eu}(\text{OTf})_3$ causes a progressive decrease of the terpyridine emission band ($\lambda_{\text{max}} = 390$ nm) with a complete disappearance achieved in correspondence of 0.5 equivalents of metal (formation of 1:2 complex, Figure 3a).

Also in this case a broad emission ligand centred band was still present. It is noteworthy that once the complex was formed, the characteristic $\text{Eu}(\text{III})$ line-like emission was clearly observed. The five sharp emission peaks at 580, 591, 617, 650 and 698 nm (inset Figure 3a), were assigned to the $^5\text{D}_0 \rightarrow ^7\text{F}_J$ ($J = 0, 1, 2, 3, 4$ and 5) transitions, with the most intense at 617 nm corresponding to the $^5\text{D}_0 \rightarrow ^7\text{F}_2$ emission. It is important to underline, that under the highly diluted conditions (10^{-7}M) employed to monitor the absorption and emission features of the **Eu@O-POSS** complex a perfectly homogeneous and transparent solution was always obtained during the titration experiments. UV-Vis absorption spectra of **O-POSS** in CH_2Cl_2 upon titration with $\text{Eu}(\text{OTf})_3$ are reported in figure S10.

This solution was characterized by a red emission evident also to the naked eyes. However, precipitation of the **Eu@O-POSS** assembled structure in the form of a pale yellow powder can be easily achieved in more concentrated solution.

Hence, solid state emission properties of the **Eu@O-POSS** complex were evaluated as well. As can be clearly seen in Figure 3b, the emission spectrum of the solid display excellent features characterized by a strong emission intensity as well as by a narrow half emission width of c.a. 10 nm. Moreover, the decrease of the intensity of the emission band of the complexed ligand suggests that the energy transfer from the terpyridine ligands to the $\text{Eu}(\text{III})$ is more efficient in the solid state. The more intense emission of **Eu@O-POSS** complex compared to the **M-POSS**-based structures can be considered as a consequence of the increased local concentration of the terpyridine surrounding the nanocage and constitute an indication of the important role played by the 3D metallopolymeric network protecting $\text{Eu}(\text{III})$ against non-radiative deactivation. These differences in the emission arising from the different environments in the assembled coordination complexes could be due to the molecular packing inducing higher emission^[20].

Once proved the emission properties of the **Eu@O-POSS** an investigation of the *trans-cis* reversible isomerization was performed. It is well known that UV light irradiation may promote *trans* to *cis* isomerization of the vinyl group. The formation of the *cis*-isomer was monitored via ^1H NMR spectroscopy selecting the **M-POSS** as target molecule. The formation of an almost equimolecular mixture of *cis* and *trans* isomers was achieved through irradiation of the *trans*-**M-POSS** at 356 nm. As can be clearly seen in Figure 4, the initial ^1H NMR spectrum displays, in the vinyl region, only one signal at 6.22 ppm (coupling constant $J = 19.1$ Hz) corresponding to the vinyl group in *trans* configuration. After irradiation, a novel signal at 5.70 ppm (coupling constant $J = 15.2$ Hz) corresponding to the *cis* form appears together with a series of signals in the aromatic part of the spectrum.

Once proved the possibility to form the *cis*-**M-POSS** structure, the *trans*-to-*cis* photoisomerization process was followed at different irradiation times via UV-visible and fluorescence spectroscopies. Upon irradiation, a decrease of the absorbance of the UV-Visible band centred at 290 nm and the concomitant appearance of a shoulder were observed (Figure S11).

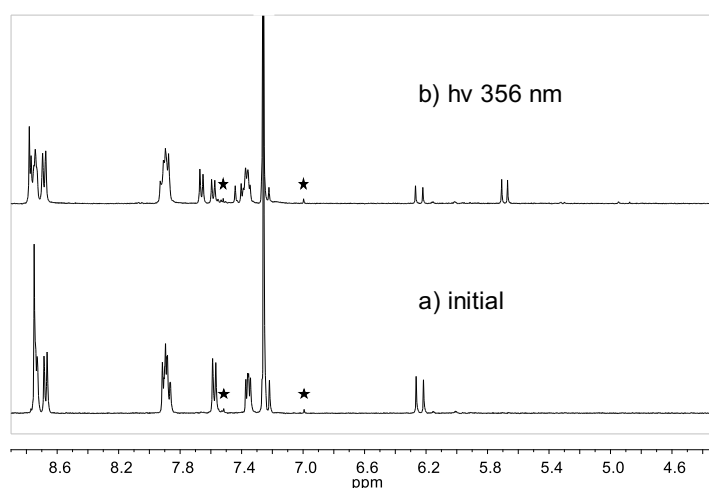


Figure 4. ^1H NMR spectrum of **M-POSS** (a) before and (b) after irradiation at 356 nm. * in the figure, indicate the ^{13}C satellites.

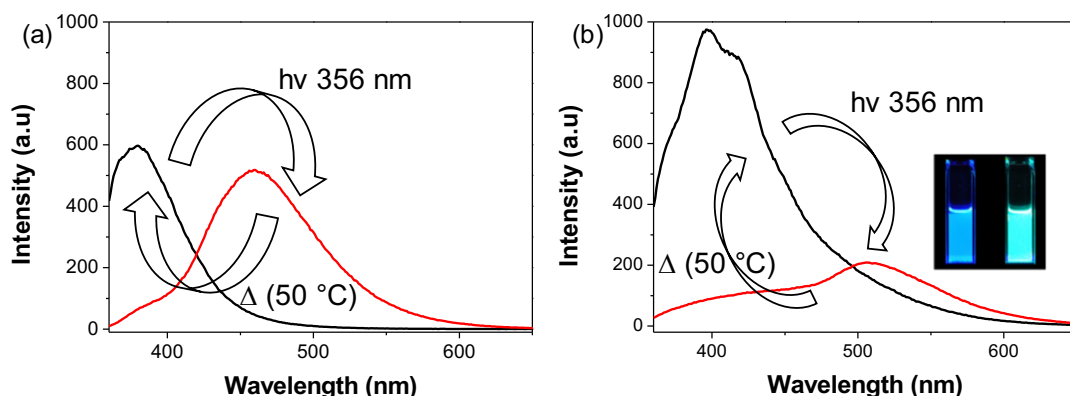


Figure 5. (a) Reversible Emission spectra of *trans*-**M-POSS** solution (black line) and *cis*-**M-POSS** (red line) (1.0×10^{-5} M) in dichloromethane registered at $\lambda_{\text{ex}} = 314$ nm slits 2.5, 5 nm (bandpass filter 360 – 1100 nm). (b) Emission spectra of **O-POSS** before and after irradiation at 356 nm. Black line: *trans*-**O-POSS** solution and red line: *cis*-**O-POSS** C = 1.2×10^{-5} M; $\lambda_{\text{ex}} = 314$ nm; slits 5, 10. Inset shows the digital photograph of the cuvette at initial and after 60 min taken under UV light at 356 nm.

A more evident transition was clearly distinguished in the fluorescent spectra. An almost complete disappearance of the emission band of *trans*-**M-POSS** at 366 nm together with the appearance of a novel emission band at 460 nm (attributed to the *cis* form) was observed after 60 minutes of irradiation at 356 nm (Figure 5). Interestingly, under the conditions employed in the fluorescence experiments, a total *trans*-to-*cis* conversion was achieved after 1h irradiation. The reversibility of the isomerization process was obtained via thermal treatment, heating the **M-POSS** solution at 50 °C during 1h (Figure 5a). Indeed, after thermal treatment at 50 °C the band at 460 nm disappeared while the contribution at 366 nm was completely restored. The process can be repeated multiple times with highly consistent results. Excitation spectra of the **M-POSS** at the maximum of the respectively emissions (370 nm for the *trans*- form and 460 nm for the *cis*- form) were recorded being practically coincident with the corresponding absorption spectra of *trans*- and *cis*- configurations respectively (Figure S13) indicating that the detected emission corresponds to the *trans*- and the *cis*- forms without observations of the excimers formation in these conditions. Analogous irradiation experiments were carried out in presence of **O-POSS**. The

photoisomerization process of **O-POSS** at different irradiation times was followed by UV-Visible and fluorescence spectroscopies. *Trans*-to-*cis* photoisomerization occurred under UV light irradiation also in presence of the **O-POSS** nanostructures. In agreement with the previously described behaviour of **M-POSS**, a decrease of the absorption band of the ligand (ca. 285 nm) and the appearance of a shoulder was observed (see Figure S14). Moreover, the emission band of the ligand was quenched almost completely and a novel broad emission band, corresponding to the *cis* form, appeared at 510 nm (Figure 5b). The broader emission band of the *cis*-**O-POSS** compared to the *trans*- isomer could be ascribed to the presence of excimers favoured by the *cis*-configuration of the double bond. Interestingly, in the case of **O-POSS** nanostructures the *trans* to *cis* isomerization was accompanied by an evident change in colour that passed from blue (*trans*-**O-POSS**) to green (*cis*-**O-POSS**). As previously observed for the **M-POSS**, also the octa-functionalized analogues display a reversible isomerization.

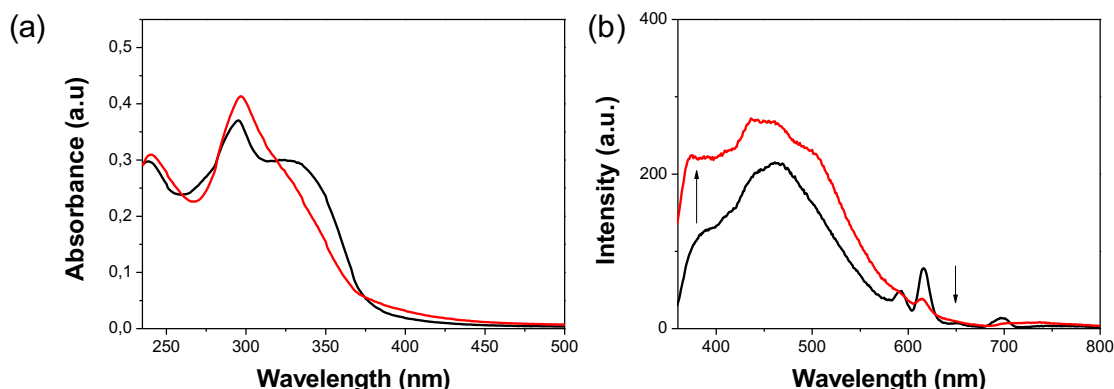
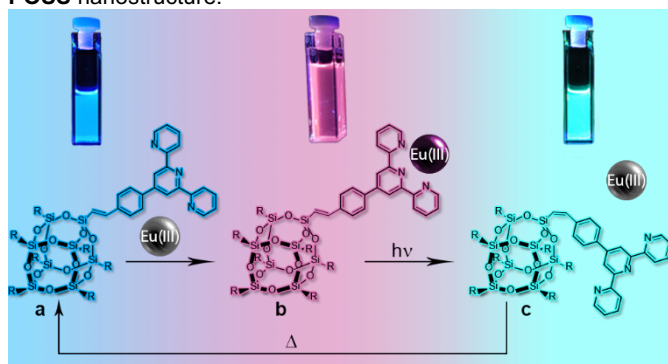


Figure 6. (a) UV-visible and (b) emission spectra of **Eu@O-POSS** (1:2) before (black line) and after irradiation (red line) at 356 nm for 60 minutes. [**O-POSS**] = 1.3×10^{-5} M; $\lambda_{\text{ex}} = 314$ nm; slits 5, 10; (bandpass filter 360 – 1100 nm).

the isomerization process of the **Eu@O-POSS** complex was followed as well via UV-Visible and fluorescence spectroscopies. It is worth highlighting that under UV irradiation the **Eu@O-POSS** complexes release almost completely the coordinated Eu(III) ions. As we can observe in the Figure 6, the characteristic Eu(III) emission bands disappeared after 1h irradiation. This behaviour can be ascribed to elevate steric hindrance of the **O-POSS** in the *cis* forms hindering the coordination of the metal centre. Changes in fluorescence emission of the **Eu@O-POSS** under UV light exposure can be detected also at naked eyes (Scheme 3). **Trans-O-POSS** (a) displays an evident blue emission, after formation of the **Eu@trans-O-POSS** complex a shift through the red is clearly observed (b), UV-irradiation of the **Eu@trans-O-POSS** causes the release of the Eu(III) ions due to the formation of the *cis*-**O-POSS** isomer whose free (non-complexed) form emits in the green (c). After thermal treatment the *cis*-**O-POSS** can be completely converted in the *trans* isomer and the cycle can be repeated without detrimental effect on **O-POSS** nanostructure.



Scheme 3. Schematic representation of the tuneable emission of (a) *trans*-**O-POSS** in dichloromethane solution; (b) **Eu@trans-O-POSS**; (c) *cis*-**O-POSS** after irradiation at 356 nm (60 minutes) under UV lamp. (R = phenyl-2,2':6',2''-terpyridine)

Moreover, in presence of small amount of solvent the **Eu@O-POSS** can be easily shaped as a film as illustrated in Figure 7. This behaviour can open the doors to application in materials science.



Figure 7. Film of the acronym of the University of Namur designed employing the *trans*-**O-POSS** (first two letters on the right), **Eu@trans-O-POSS** (letters in the middle) and *cis*-**O-POSS** (last two letters on the right) under UV lamp (356 nm).

Conclusions

The adsorption and emission properties of two novel silsesquioxane-based Eu complexes were investigated. The stoichiometry of the complexes (**Eu@2M-POSS** and **Eu@2O-POSS**) was evaluated via ^1H NMR as well as UV-Vis and fluorescence titration experiments. The solutions of **Eu@2O-POSS** display a bright-red luminescence under UV light at room temperature and an even more intense emission can be achieved in solid state. Interestingly both **M-** and **O-POSS** nanostructures display a reversible *trans* to *cis* isomerization of the carbon-carbon double bond linking the silsesquioxane core to the terpyridine moieties. In the case of **O-POSS** nanocages this isomerization was monitored also in presence of Eu(III) cations and was accompanied by an evident modification of the colour which passed from blue (*trans*-**O-POSS**) to red (**Eu@trans-O-POSS**) and finally to green (*cis*-**O-POSS**) as consequence of the release of the metal cations. After thermal treatment, the *cis*-**O-POSS** can be completely converted in the *trans* isomer and the cycle can be repeated without detrimental effect on **O-POSS** nanostructure. This switchable and reversible “blue-red-green” emission together with the easy dispersion and the possibility of forming films makes the emitting solid promising for applications in materials science and in particular in the preparation of advanced light emitting devices.

Experimental Section

Materials and method: Monovinyl-isobutyl substituted POSS (MV), Octavinyl POSS (OV), DMF anhydrous, Et₃N (99.5%), Eu(III) triflate (99.999%) were purchased from Sigma Aldrich. 4'-(4-Bromophenyl)-2,2':6',2''-terpyridine, palladium acetate, tris(2-methylphenyl)phosphine were purchased from TCI chemicals. Acetonitrile (CH₃CN) and dichloromethane (DCM) used for the spectrofluorometric measurements were of spectroscopic grade and these were purchased from Carl Roth. Quantitative ^1H NMR experiments were performed at 25 °C on a Varian VNMRs spectrometer. UV-visible measurements were performed on Cary 5000 Spectrophotometer (Varian) and fluorescent measurements on Cary Eclipse (Agilent technologies). The measurements were carried out using 10 mm suprasil quartz cuvettes from Hellma Analytics. Irradiation test were performed with an ASASHI SPECTRA Xenon Light Source 300W MAX-303.

Synthesis M-POSS: To an oven-dried, double neck 50 mL flask under flowing N₂, 400 mg of MV (0.42 mmol), 10.8 mg of palladium acetate, 29.2 mg of tris(2-methylphenyl)phosphine (0.096 mmol), 280 mg of 4'-(4-bromophenyl)-2, 2':6', 2''-terpyridine (0.72 mmol), 14 mL of DMF anhydrous and 4 mL of Et₃N were added. The reaction mixture was heated at 100 °C for 3 days under N₂ atmosphere. After that, the mixture was cooled at room temperature and filtered to remove the palladium metal. The filtrate was cooled down precipitating the **M-POSS**.

M-POSS, white powder. **Yield: 80 %**. ^1H -NMR (400 MHz, CDCl₃) δ (ppm) = 0.69-0.62 (m, 14H), 0.95-1.00 (m, 42H), 1.81-1.95 (m, 7H), 6.27-6.22 (d, 1H), 7.27-7.22 (d, 1H), 7.37-7.34 (t, 2H), 7.59-7.57 (d, 1H), 7.92-7.86 (m, 4H), 8.69-8.67 (d, 2H), 8.74-8.73 (d, 2H), 8.75 (s, 2H). ^{13}C -NMR (100 MHz, CDCl₃) δ (ppm) = 22.60, 23.96, 25.82, 118.77, 119.81, 121.47, 123.96, 127.43, 127.61, 136.99, 138.39, 138.65, 147.38, 149.24, 149.77, 156.06, 156.30. MAS ^{29}Si -NMR (99.3 MHz) δ (ppm) = -68.27, -80.17. Elemental analysis (%) for C₅₁H₇₉N₃O₁₂Si₈; calculated: C= 53.23, H= 6.92, N= 3.65; found: C= 52.45, H= 6.79, N= 3.22.

Synthesis O-POSS: To an oven-dried, double neck 50 mL flask under flowing N₂, 135 mg of OV (0.21 mmol), 20.8 mg of palladium acetate (0.09 mmol), 58 mg of tris(2-methylphenyl)phosphine (0.018 mmol), 1 g

of 4'-(4-bromophenyl)-2, 2':6', 2"-terpyridine (2.57 mmol), 14 mL of DMF anhydrous and 4 mL of Et₃N were added. The reaction mixture was heated at 100 °C for 7 days under N₂ atmosphere. After that, the mixture was cooled and filtered to remove the Pd⁰ and then precipitated in 50 mL of deionized water. The precipitate was, for first, washed with water (2 x 25 ml) sonicating in a bath and centrifuging 10 minutes at 4500 rpm. The same procedure was repeated washing the solid with acetonitrile (5 x 25 ml), then with methanol (5 x 25 ml) and finally with acetone (2 x 25mL). **O-POSS** was obtained as a pale brown powder. Yield: 68 %. MAS ²⁹Si NMR (99.3 MHz) δ (ppm) = -80.29. Elemental analysis (%) for C₅₁H₇₉N₃O₁₂Si₈; calculated: C= 71.48, H= 4.17, N= 10.87; found: C= 67.04, H= 3.99, N= 9.78.

Synthesis Eu@2O-POSS: In a single-neck 50 mL flask 50 mg of O-POSS (0.016 mmol), 39 mg of Eu (III) triflate (0.065 mmol) and 20 mL of a mixture of DCM and CH₃CN (65%:35%) were added. The mixture was cooled at 50°C for 24h. After this time, the volume of the mixture was reduced by evaporation under reduced pressure and a pale yellow precipitate was collected under vacuum. The solid was washed on the filter with DCM and CH₃CN and dried under vacuum.

Irradiation procedure: Irradiation tests for ¹H-NMR were performed in "5mm Thin Wall Natural Quartz NMR Sample Tubes" from NORELL. Absorption and emission experiments were performed in 10 mm suprasil quartz cuvettes from Hellma Analytics. All the irradiation tests were carried out by placing the samples at a distance of 21 cm from the UV source.

Acknowledgements

The authors acknowledge the University of Palermo and the University of Namur. V.C. gratefully acknowledges the University of Palermo and University of Namur for a co-funded PhD fellowship.

Keywords: keyword 1 • keyword 2 • keyword 3 • keyword 4 • keyword 5

- [1] P. P. Pescarmona, C. Aprile, S. Swaminathan, in *New and Future Developments in Catalysis* (Ed.: S. L. Suib), Elsevier, 2013.
- [2] aR. Duchateau, W. J. van Meerendonk, S. Huijser, B. B. P. Staal, M. A. van Schilt, G. Gerritsen, A. Meetsma, C. E. Koning, M. F. Kemmere, J. T. F. Keurentjes, *Organometallics* 2007, 26, 4204-4211; bR. Kunthom, T. Jaroentomeechai, V. Ervithayasuporn, *Polymer* 2017, 108, 173-178; cK. Wada, M. Nakashita, T. Mitsudo, *Chem. Commun.* 1998, 133-134.
- [3] aR. Y. Kannan, H. J. Salacinski, J.-e. Ghanavi, A. Narula, M. Odlyha, H. Peirovi, P. E. Butler, A. M. Seifalian, *Plast. Reconstr. Surg.* 2007, 119, 1653-1662; bS. B. Rizvi, S. Y. Yang, M. Green, M. Keshtgar, A. M. Seifalian, *Bioconjugate Chem.* 2015, 26, 2384-2396; cC. Zhang, F. Babonneau, C. Bonhomme, R. M. Laine, C. L. Soles, H. A. Hristov, A. F. Yee, *J. Am. Chem. Soc.* 1998, 120, 8380-8391.
- [4] L. A. Bivona, O. Fichera, L. Fusaro, F. Giacalone, M. Buaki-Sogo, M. Gruttadauria, C. Aprile, *Catal. Sci. Technol.* 2015, 5, 5000 - 5007
- [5] aL. A. Bivona, F. Giacalone, E. Carbonell, M. Gruttadauria, C. Aprile, *ChemCatChem* 2016, 8, 1685-1691; bC. Calabrese, L. F. Liotta, F. Giacalone, M. Gruttadauria, C. Aprile, *ChemCatChem*, 0.
- [6] A. Tsuchida, C. Bolln, F. G. Sernetz, H. Frey, R. Mülhaupt, *Macromolecules* 1997, 30, 2818-2824.
- [7] C. Hartmann-Thompson, D. L. Keeley, K. M. Pollock, P. R. Dvornic, S. E. Keinath, M. Dantus, T. C. Gunaratne, D. J. LeCaptain, *Chem. Mater.* 2008, 20, 2829-2838.
- [8] G. H. Mehl, I. M. Saez, *Appl. Organomet. Chem.* 1999, 13, 261-272.
- [9] E. Carbonell, L. A. Bivona, L. Fusaro, C. Aprile, *Inorg. Chem.* 2017, 56, 6393-6403.
- [10] C.-C. Cheng, Y.-L. Chu, C.-W. Chu, D.-J. Lee, *J. Mater. Chem. C* 2016, 4, 6461-6465.
- [11] P. Escribano, B. Julián-López, J. Planelles-Aragó, E. Cordoncillo, B. Viana, C. Sanchez, *J. Mater. Chem.* 2008, 18, 23-40.
- [12] S. S. Syamchand, G. Sony, *J. Lumin.* 2015, 165, 190-215.
- [13] aU. S. Schubert, A. Winter, G. R. Newkome, in *Terpyridine-Based Materials*, Wiley-VCH Verlag GmbH & Co. KGaA, 2011, pp. 129-197; bO. Kotova, S. Comby, C. Lincheneau, T. Gunnlaugsson, *Chem. Sci.* 2017, 8, 3419-3426.
- [14] V. Bekiari, P. Lianos, *J. Lumin.* 2003, 101, 135-140.
- [15] aJ. W. Chung, S.-J. Yoon, B.-K. An, S. Y. Park, *J. Phys. Chem. C* 2013, 117, 11285-11291; bC. Dugave, L. Demange, *Chem. Rev.* 2003, 103, 2475-2532.
- [16] P. P. Lima, M. M. Nolasco, F. A. A. Paz, R. A. S. Ferreira, R. L. Longo, O. L. Malta, L. D. Carlos, *Chem. Mater.* 2013, 25, 586-598.
- [17] L.-R. Lin, H.-H. Tang, Y.-G. Wang, X. Wang, X.-M. Fang, L.-H. Ma, *Inorg. Chem.* 2017, 56, 3889-3900.
- [18] aM. Bian, Y. Wang, X. Guo, F. Lv, Z. Chen, L. Duan, Z. Bian, Z. Liu, H. Geng, L. Xiao, *J. Mater. Chem. C* 2018, 6, 10276-10283; bD. Zych, A. Slodek, M. Matussek, M. Filapek, G. Szafraniec-Gorol, S. Krompiec, S. Kotowicz, M. Siwy, E. Schab-Balcerzak, K. Bednarczyk, M. Libera, K. Smolarek, S. Maćkowski, W. Danikiewicz, *ChemistrySelect* 2017, 2, 8221-8233.
- [19] H.-L. Au-Yeung, S. Y.-L. Leung, A. Y.-Y. Tam, V. W.-W. Yam, *J. Am. Chem. Soc.* 2014, 136, 17910-17913
- [20] aJ. Andres, A.-S. Chauvin, *Eur. J. Inorg. Chem.* 2010, 2700-2713; bV. Divya, R. O. Freire, M. L. P. Reddy, *Dalton Trans.* 2011, 40, 3257-3268; cZ.-M. Zhang, F.-F. Han, R. Zhang, N. Li, Z.-H. Ni, *Tetrahedron Lett.* 2016, 57, 1917-1920.

